



DOI:10.22144/ctujoisd.2025.001

## Multi-Quality Optimization in Pulsed Laser Cutting of Thin Laminated Cores Using the Preference Selection Index Method

Nguyen Van Tai<sup>1</sup>, Nguyen Van Cuong<sup>1</sup>, Huynh Thanh Thuong<sup>1</sup>, Nguyen Dinh Tu<sup>2</sup>,  
Nguyen Thi Kim Khanh<sup>1</sup>, Ho Jeng-Rong<sup>3</sup>, and Nguyen Hoai Tan<sup>1\*</sup>

<sup>1</sup>Faculty of Mechanical Engineering, Can Tho University, Viet Nam

<sup>2</sup>Faculty of Mechanical Engineering, Can Tho University of Technology, Viet Nam

<sup>3</sup>Department of Mechanical Engineering, National Central University, Taiwan

\*Corresponding author (nhtan@ctu.edu.vn)

### Article info.

Received 18 Jul 2024  
Revised 21 Aug 2024  
Accepted 23 Jan 2025

### Keywords

Preference selection index (PSI) method, pulse laser cutting, recast layer, surface roughness, thin electrical steel

### ABSTRACT

This study explores a pulsed Nd:YAG laser cutting of thin laminated cores made from non-oriented electrical steel sheets, aiming to optimize cutting quality aims to investigate the cutting quality of a thin laminated core using a non-oriented electrical steel sheet by a pulsed fiber Nd: YAG laser. The influence of laser power ( $P$ ), scanning speed ( $v$ ), and pulse repetition rate ( $f$ ) on cutting time ( $T_C$ ), recast layer height ( $H$ ), and kerf surface roughness ( $S_a$ ) is analyzed to determine optimal processing parameters. Each process parameter is elected with three levels, and a total of 27 experimental datasets are achieved. The preference selection index (PSI) method is used to determine the optimal cutting quality based on multiple criteria derived from experimental results. The best quality is found at No. 23 with process parameters of  $P = 18$  W,  $v = 600$  mm/s, and  $f = 30$  kHz for qualities of  $T_C = 20.6$  s,  $H = 20.2$   $\mu$ m, and  $S_a = 2.4$   $\mu$ m.

## 1. INTRODUCTION

Electrical steel (ESs) is the most useful in the electrical industry, such as the stator core of electric motors, generators, and transformers, due to its excellent magnetic properties. In industrial manufacturing, punching and/or stamping are the most common process for cutting electrical steel; however, the mechanical process will affect the deterioration of the magnetic properties of ESs, especially on thin sheets, due to the changing grain size or/and orientation, deforming strip thickness (Emura et al., 2003; Naumoski et al., 2015). Recently, pulsed laser cutting has become a promising alternative for cutting the ESs due to the non-nature contact for solving problems of mechanical cutting and the cost of the cutting tools.

In the field of laser cutting, a common area of research is the interconnected effect of key input process parameters (laser power, cutting speed, pulse repetition rate, and focal position) on cut quality. These output qualities include the heat-affected zone (Siebert et al., 2014; Nguyen et al., 2020), kerf characteristics, and surface roughness (Madić et al., 2012). Essentially, researchers investigate how manipulating the laser's power, the speed of the cut, the frequency of laser pulses, and the focus of the laser beam impacts the extent of heat influence on the material, the width and shape of the cut, and the smoothness of the cut edge. The pulsed Nd: YAG laser is proposed for cutting thin material because Nd: YAG laser leads to a smaller thermal load in cutting which results in a narrow kerf and small heat-affected zone as compared to the CO<sub>2</sub> laser (Naumoski et al., 2015).

Motors/rotors/ stators are typically constructed from hundreds or thousands of core laminations. Therefore, the morphology and dimensions of each individual lamination play a significant role in the assembly process. The dross/debris/recast layer that causes the deterioration in the magnetic property of electrical steel remains at the cut edge after the laser cutting. In addition, the time required to complete a core lamination cut is critical to mass production. Due to the joint effects of process parameters and qualities, the Preference Selection Index method is a good tool for selecting the best alternative from given alternatives without deciding the relative importance between attributes (Miloš et al., 2017; Haoues et al., 2023; Nguyen et al., 2024)

Thin electrical steel sheets (ESs) are advantageous for energy savings and miniaturization of high-repetition-rate reactors, transformers, and motors due to their inherent characteristics of low core loss, high flux density, and high permeability. Thus, this study targets thin ESs with a thickness of 0.1 mm by pulse laser cutting of core lamination. The main purpose here is to obtain the joint effects of process parameters which are laser power ( $P$ ), scanning speed ( $v$ ), and pulse repetition rate ( $f$ ) on the three cutting qualities that involve cutting time, height of

recast layer, and surface roughness. The experimental results are presented and the relationships between the cutting qualities and the process parameters are discussed. Finally, the PSI method is used to determine the best quality with a process parameter.

## 2. RESEARCH METHODOLOGY

### 2.1. Experimental procedure

In this experimental study, 80 mm diameter laminated cores were fabricated by cutting 0.1 mm thick, non-oriented electrical steel sheets (ST-100, Nikkendenji Kogyo Co., Ltd). A pulsed fiber laser system (IPG YLP-1-100-20-20) was used for the cutting. The laser head has a wavelength of 1070 nm and operate with maximum power of 20 W at 100 ns pulse duration. As shown in Fig. 1, the laser beam has a spot diameter of 40  $\mu\text{m}$ , a scanner field of 110 x 110 mm, and a focal distance of 127 mm. The spacers and holders are used to avoid possible uneven heat accumulation and have a uniform cutting quality. The three input process parameters are  $P$ ,  $v$ , and  $f$ , with three levels as presented in Table 1, considering investigating their influences on cutting time ( $T_C$ ), height of recast layer ( $H$ ), and surface roughness ( $S_a$ ).

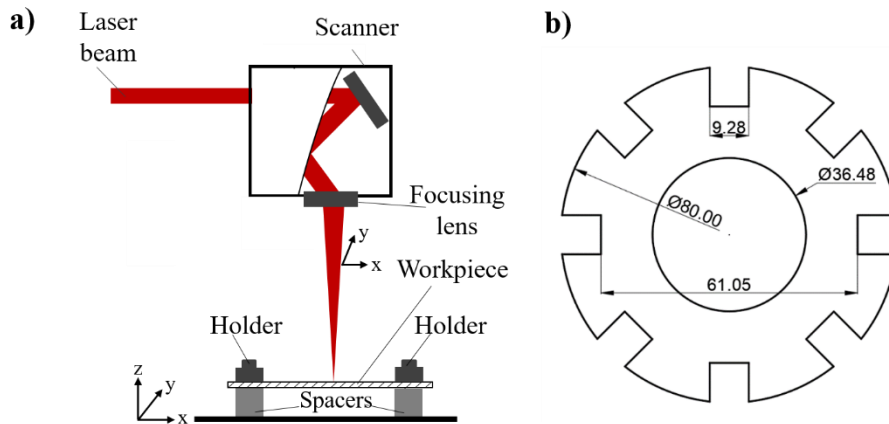


**Fig. 1. (a) A schematic diagram of the experimental arrangement used in this study; and (b) the dimensions of an 80 mm diameter motor laminated core produced in this work**

The cutting time,  $T_C$ , refers to the required time for achieving a through cut of a laminated core with 513 mm of total kerf-length, calculated by Eq. (1) with intervals of 1 ms.

$$T_C = \text{Scan times} \cdot \left( \frac{\text{Total length}}{\text{Scanning speed}} \right) + (\text{Scan times} - 1) \cdot \text{Interval time} \quad (1)$$

**Table 1. Laser processing parameters and values**

Process parameters	Levels		
	1	2	3
Laser power, $P$ (W)	10	14	18
Scanning speed, $v$ (mm/s)	400	600	800
Pulse repetition rate, $f$ (kHz)	20	30	40

To measure the height of the recast layer and surface roughness, the cut workpiece must be cleaned in ultrasound with isopropanol for 30 minutes. The measurement is taken based on the image of 20 locations, along with the lamination by a laser confocal microscope (KEYENCE VK-X1000). The surface roughness in the area is measured in 20 positions of the cut-view with the area 90 x 90 μm.

**2.2. Preference selection index (PSI) method**

The PSI method, proposed by Maniya and Bhatt (Maniya et al., 2010), offers a solution to complex decision-making in uncertain environments. A key feature of this method is its ability to calculate criteria weights based solely on the data within the decision matrix, thus avoiding the need to specify the relative importance of the criteria. In this study, the good cutting qualities through minimizing the cutting time are pointed out. That means minimization of cutting time ( $T_C$ ), height of recast layer ( $H$ ) and surface roughness ( $S_a$ ). As in the definition of the PSI method, the-larger-the-better is the expected value. The combination of the objective function  $J$  is to achieve maximization as given in Eq. (2)

$$J = w_1 \cdot \frac{T_{Cmin}}{T_C} + w_2 \cdot \frac{H_{min}}{H} + w_3 \cdot \frac{S_{amin}}{S_a} \quad (2)$$

a) Identification and selection of relevant criteria for alternative evaluation;

b) Development of the initial decision matrix  $Y$  for alternative assessment,

$$Y = Y_{ij} = \begin{bmatrix} y_{11} & y_{12} & \dots & y_{1n} \\ y_{21} & y_{22} & \dots & y_{2n} \\ \dots & \dots & \dots & \dots \\ y_{m1} & y_{m2} & \dots & y_{mn} \end{bmatrix},$$

where  $i = 1, 2, \dots, m$  for number of alternative; and  $j = 1, 2, \dots, n$  for number of criteria. In this study,  $m$  is 27, and  $n$  is 3;

c) Normalization of the data for each characteristic, for minimization,

$$R_{ij} = y_{ij}^{min} / y_{ij}$$

d) Calculation the mean values of each output,

$$N = (\sum_{i=1}^m R_{ij}) / n$$

e) Determination of the variable values for each quality,

$$\phi_j = \sum_{i=1}^m (R_{ij} - N)^2$$

f) Computing the deviations with each output using the equation:

$$\Omega_j = 1 - \phi_j$$

g) Obtaining the weighting for each criterion

$$w_j = \Omega_j / \sum_{j=1}^n \Omega_j, j = 1, 2, \dots, n$$

where  $w_1$ ,  $w_2$ , and  $w_3$  represent the weights associated with characteristics of  $T_C$ ,  $H$ , and  $S_a$ , respectively.

**3. RESULTS AND DISCUSSION**

As indicated in Table 2, a total of 27 experimental cases are presented. Based on the experimental data, a discussion and demonstration of the effects of process parameters on cutting quality are provided. Fig. 2 demonstrates the cutting time as a function of process parameters. Fig. 2a shows that, while the other two process parameters,  $f$ , and  $v$ , are fixed,  $T_C$  decreased with the increase of  $P$ . Since ablation is the main mechanism for the thin ESs laser cutting, the higher the laser power, the shorter the cutting time. When the scan speed is fixed, Fig. 2b shows the cutting time increases with the increase of pulse repetition rate at the same powers. At the fixed scan speed and under the same power, the fluence remains unchanged. The pulse overlapping, however, still increases with the increase of pulse repetition rate. From the experimental dataset shown in Table 2, the minimum cutting time is 18.0 s, which occurred in case No. 19, where the process parameters are  $P = 18$  W,  $v = 400$  mm/s, and  $f = 20$  kHz.

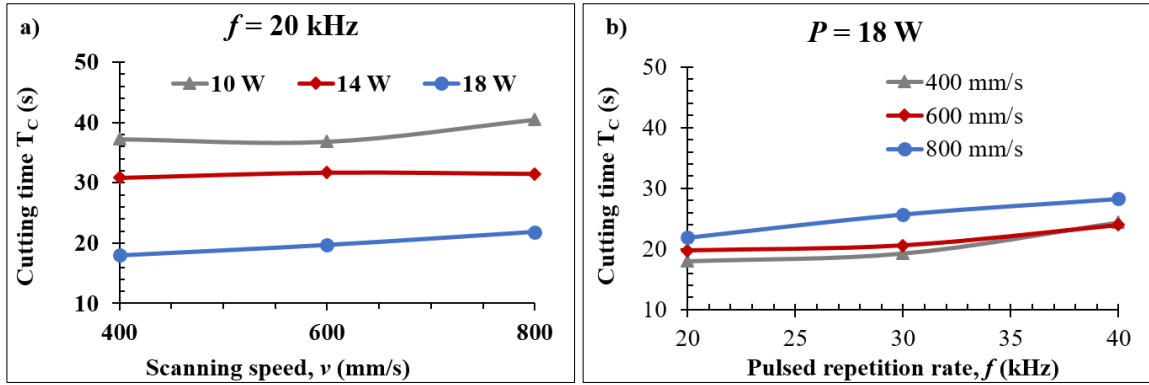


Fig. 2. The relationship between process parameters and cutting time ( $T_c$ )

Table 2. All 27 experimental cases and results

No.	Input parameters			Output qualities		
	Power, $P$ (W)	Scanning speed, $v$ (mm/s)	Pulse repetition rate, $f$ (kHz)	Cutting time $T_c$ (s)	Height of recast layer $H$ ( $\mu\text{m}$ )	Surface roughness $S_a$ ( $\mu\text{m}$ )
1	10	400	20	27.3	29.8	3.1
2	10	400	30	36.8	28.8	2.2
3	10	400	40	40.5	26.1	3.1
4	10	600	20	30.8	18.6	2.7
5	10	600	30	33.4	12.3	1.6
6	10	600	40	36.6	6.3	2.3
7	10	800	20	30.8	10.4	2.7
8	10	800	30	31.7	8.3	2.2
9	10	800	40	32.1	5.1	2.1
10	14	400	20	30.8	46.9	3.0
11	14	400	30	31.7	38.2	2.6
12	14	400	40	31.5	36.1	3.3
13	14	600	20	27.0	37.5	2.8
14	14	600	30	40.3	33.0	2.0
15	14	600	40	31.5	16.3	3.1
16	14	800	20	25.7	13.1	3.1
17	14	800	30	25.7	12.8	2.7
18	14	800	40	27.6	7.5	2.1
19	18	400	20	18.0	53.0	3.4
20	18	400	30	19.7	42.6	3.1
21	18	400	40	21.9	38.5	3.2
22	18	600	20	19.3	16.9	2.9
23	<b>18</b>	<b>600</b>	<b>30</b>	<b>20.6</b>	<b>20.2</b>	<b>2.4</b>
24	18	600	40	25.7	17.1	2.7
25	18	800	20	24.4	25.9	3.1
26	18	800	30	24.0	23.4	2.9
27	18	800	40	28.3	21.3	2.8
Min	<b>10</b>	<b>400</b>	<b>20</b>	<b>18.0</b>	<b>5.1</b>	<b>1.6</b>
Max	<b>18</b>	<b>800</b>	<b>40</b>	<b>40.5</b>	<b>53.0</b>	<b>3.4</b>

Fig. 3 presents the effects of cutting parameters on the height of the recast layer. The recast layer thickness is increased by increasing laser power, a result of the greater laser energy ablation on the workpiece (Ghany et al., 2001). However, the rising

of scanning speed slightly reduces the recast layer and considerably drops by the rise in pulse repetition rate. Fig. 3c and Fig. 3d show the OM images of the lowest and highest of recast layers with  $5.12 \mu\text{m}$  at No. 9 and  $53.07 \mu\text{m}$  at No. 19, respectively.

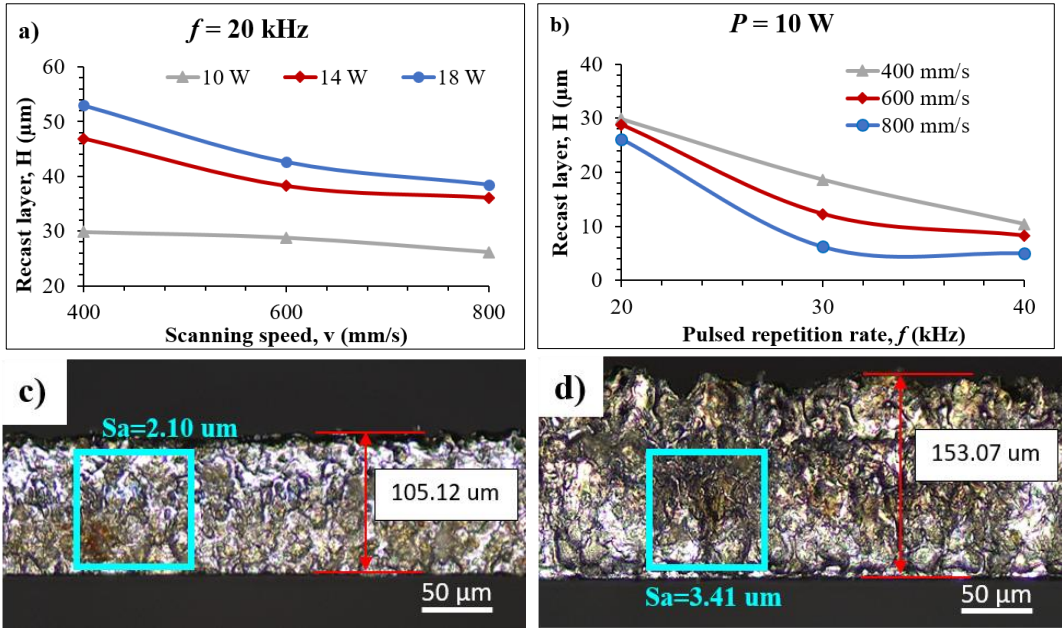


Fig. 3. Effects of process parameters on the height of recast layer (H) for a) and b). OM images of the side view and surface roughness of cutting at No. 9 for c) and No. 19 for d).

Fig. 4 shows the surface roughness variation with scanning speed under various powers but at a fixed pulse repetition rate of 20 kHz. A higher laser power results in a faster material removal rate and introduces a greater surface roughness and slightly decreases with the increase of  $v$ , as observed in (Ghany et al., 2001). At a fixed power of 10 W,  $S_a$  slightly drops with the increase of  $f$ , and for the

higher pulse repetition rate part,  $S_a$  rises with the increase of  $f$ . Due to the pulse overlapping increase with the increase of pulse repetition rate that usually improves the surface roughness. The OM images and corresponding partial, three-dimensional surface morphology are shown in Fig. 4c and Fig. 4d.

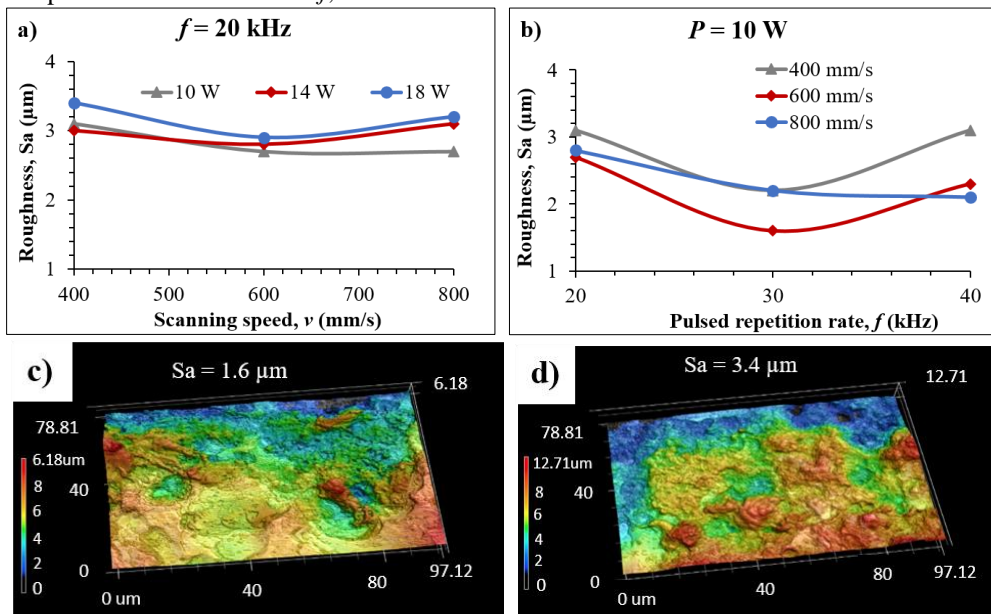


Fig. 4. Effects of process parameters on the surface roughness,  $S_a$  for a) and b). Characterizing kerf surface roughness at No. 5 for c) and No. 19 for d).

**Table 3. Normalize the data for three qualities,  $R_{ij}$**

No.	Normalization		
	$T_C$ (s)	H ( $\mu\text{m}$ )	$S_a$ ( $\mu\text{m}$ )
1	0.4827	0.1711	0.5161
2	0.4882	0.1771	0.7273
3	0.4441	0.1954	0.5161
4	0.5833	0.2742	0.5926
5	0.5382	0.4146	1.0000
6	0.4908	0.8095	0.6957
7	0.5833	0.4904	0.5926
8	0.5673	0.6145	0.7273
9	0.5596	1.0000	0.7619
10	0.5833	0.1087	0.5333
11	0.5673	0.1335	0.6154
12	0.5710	0.1413	0.4848
13	0.6667	0.1360	0.5714
14	0.4466	0.1545	0.8000
15	0.5710	0.3129	0.5161
16	0.7000	0.3893	0.5161
17	0.6997	0.3984	0.5926
18	0.6506	0.6800	0.7619
19	1.0000	0.0962	0.4706
20	0.9127	0.1197	0.5161
21	0.8229	0.1325	0.5000
22	0.9333	0.3018	0.5517
23	0.8747	0.2525	0.6667
24	0.6994	0.2982	0.5926
25	0.7368	0.1969	0.5161
26	0.7497	0.2179	0.5517
27	0.6359	0.2394	0.5714
<b>N</b>	<b>5.8531</b>	<b>2.8189</b>	<b>5.4861</b>

Based on the procedure in the §2.2 section, the computation of weights for the PSI method is expressed and calculated, as presented in Table 3 and Table 4. Firstly, the goal and relevant criteria are identified and selected, and the initial decision matrix Y of output qualities are developed. Then, the mean value of the normalized performance for each quality characteristic, N, is calculated after the minimal normalization of the datasets as 5.8531 for  $T_C$ , 2.8189 for H, and 5.4861 for  $S_a$ , respectively.

The computational values for  $\phi$ ,  $\Omega$  of the three qualities was expressed in Table 4. The variable values,  $\phi$  of preferences, were determined for each output characteristic as 731.4454 for  $T_C$ , 170.8817 for H, and 642.4633 for  $S_a$ . First of all, the preference deviation values for each characteristic were calculated. These deviations were -730.4454 for  $T_C$ , -169.8816 for H, and -641.4632 for  $S_a$ . The

total deviation across all three was  $\Omega = 1541.7902$ . Next, each characteristic was assigned a weight reflecting its importance.  $T_C$  received a weight of  $w_1 = 0.4738$ , H a weight of  $w_2 = 0.1102$ , and  $S_a$  a weight of  $w_3 = 0.4161$ . These weights were incorporated into Eq. (2) to create a single score (J) representing the overall system performance. The various configurations (cases) revealed that Case No. 23 yielded the highest score ( $J = 0.7196$ ), signifying the best outcome. Conversely, Case No. 3 had the lowest score ( $J = 0.4467$ ), representing the worst performance. Therefore, Case No. 23 offers the most desirable balance of  $T_C$ , H, and  $S_a$ .

**Table 4. Computational values of PSI**

No.	Computational values of PSI				
	$T_C$ (s)	H ( $\mu\text{m}$ )	$S_a$ ( $\mu\text{m}$ )	J Ranking	
1	28.8403	7.0107	24.7005	0.4623	26
2	28.7821	6.9792	22.6464	0.5534	20
<b>3</b>	<b>29.2570</b>	<b>6.8828</b>	<b>24.7005</b>	<b>0.4467</b>	<b>27</b>
4	27.7702	6.4756	23.9463	0.5531	21
5	28.2474	5.7805	20.1250	0.7167	2
6	28.7535	4.0376	22.9483	0.6112	11
7	27.7702	5.4220	23.9463	0.5769	16
8	27.9389	4.8596	22.6464	0.6391	8
9	28.0213	3.3084	22.3180	0.6923	5
10	27.7702	7.3450	24.5298	0.5102	24
11	27.9389	7.2114	23.7238	0.5395	22
12	27.9005	7.1697	25.0124	0.4878	25
13	26.8988	7.1980	24.1539	0.5686	17
14	29.2296	7.0988	21.9595	0.5615	19
15	27.9005	6.2802	24.7005	0.5197	23
16	26.5542	5.9029	24.7005	0.5893	14
17	26.5570	5.8587	23.9463	0.6220	9
18	27.0652	4.5749	22.3180	0.7002	4
19	23.5522	7.4130	25.1553	0.6802	6
20	24.4073	7.2856	24.7005	0.6603	7
21	25.3027	7.2170	24.8611	0.6125	10
22	24.2038	6.3360	24.3480	0.7050	3
<b>23</b>	<b>24.7846</b>	<b>6.5866</b>	<b>23.2269</b>	<b>0.7196</b>	<b>1</b>
24	26.5598	6.3537	23.9463	0.6108	12
25	26.1758	6.8749	24.7005	0.5855	15
26	26.0443	6.7650	24.3480	0.6087	13
27	27.2192	6.6537	24.1539	0.5654	18
$\phi_j$	731.4454	170.8817	642.4633		
$\Omega$	-	-	-		
$w_j$	0.4738	0.1102	0.4161		

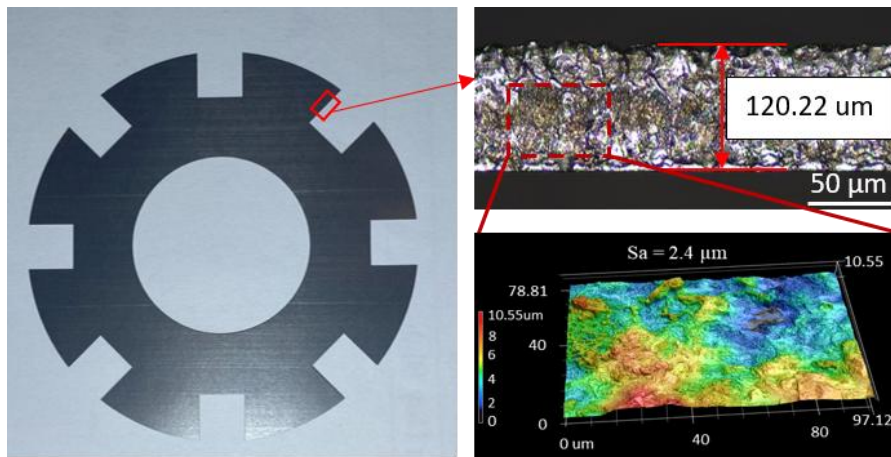


**Fig. 5. (a) High-quality laminated core cut based on PSI optimization (Case No. 23:  $P = 18$  W,  $v = 600$  mm/s,  $f = 30$  kHz). (b) Optical microscope (OM) image of a tooth's side view. (c) Surface roughness analysis**

Fig. 5 presents the laminated core-cut with the best quality for  $T_C$  of 20.6 s,  $H$  of 20.2  $\mu\text{m}$  and  $S_a$  of 1.6  $\mu\text{m}$ . Compared to No. 23, No. 5 also obtains the second-best quality. Case 5 presented better quality for the recast layer of  $H = 12.3$   $\mu\text{m}$  and surface roughness of  $S_a = 1.6$   $\mu\text{m}$  than case No. 23; however, the cutting time is longer 33.4 s.

#### 4. CONCLUSION

In this study, a laminated core shape with a diameter of 80 mm made by thin ESs was cut by a pulsed Nd: YAG laser system. The cutting process was investigated to evaluate the influences of the three parameters that are laser power, scanning speed, and pulse repetition rate on three cutting qualities (cutting time, the height of the recast layer, and surface roughness). Each process parameter had three levels: laser power (10, 14, and 18 W), scanning speed (400, 600, and 800 mm/s), and pulse repetition rate (20, 30, and 40 kHz).

#### REFERENCES

- Emura, M., Landgraf, F. J. G., Ross, W., & Barreta, J. R. (2003). The influence of cutting technique on the magnetic properties of electrical steels. *Journal of Magnetism and Magnetic Materials*, 254, 358-360.
- Naumoski, H., Riedmüller, B., Minkow, A., Herr, U. (2015). Investigation of the influence of different cutting procedures on the global and local magnetic properties of non-oriented electrical steel. *Journal of Magnetism and Magnetic Materials*, 392, 126-133.
- Siebert, R., Schneider, J., Beyer, E. (2014). Laser cutting and mechanical cutting of electrical steels and its effect on the magnetic properties. *IEEE Transaction Magnetic*, 50, 2001904.
- Nguyen, T.H., Lin, C.K., Tung, P.C., Cuong, N.V., Ho, J.R. (2020). An extreme learning machine for predicting kerf waviness and heat affected zone in pulsed laser cutting of thin non-oriented silicon steel. *Optics and Lasers in Engineering*, 134, 106244.
- Madić, M., Radovanović, M., Nedić B. (2012). Correlation between surface roughness characteristics in  $\text{CO}_2$  laser cutting of mild steel. *Tribology in Industry*, 34, 232-238.
- Nguyen, T.H., Lin, C.K., Tung, P.C., Cuong, N.V., Ho, J.R. (2024). Manufacturing motor core lamination from thin non-oriented silicon steel sheet direct by pulsed laser. cutting using multi-quality optimized

- process parameters. *The International Journal of Advanced Manufacturing Technology*, 133, 199-220.
- Miloš, M., Antucheviciene, J., Radovanović, M., Petković D. (2017). Determination of laser cutting process conditions using the preference selection index method. *Optics and Laser Technology*, 89, 214-220.
- Haoues, S., Yaltese, MA., Belhadi, S., Chihaoui, S., Uysal, A. (2023). Modeling and optimization in turning of PA66-GF30% and PA66 using multi-criteria decision-making (PSI, MABAC, and MAIRCA) methods: a comparative study *The International Journal of Advanced Manufacturing Technology*, 124(7-8), 2401-2421.
- Maniya, K., Bhatt, MG. (2010). A selection of material using a novel type decision-making method: Preference selection index method. *Materials and Design*, 31, 1785-1789.
- Ghany, KA., Newishy, M. (2001). Cutting of 1.2 mm thick austenitic stainless steel sheet using pulsed and CW Nd: YAG laser. *The Journal of Materials Processing Technology*, 168, 438-447.